Scientific Research Publishing

Combining Self-Organizing Map and Lipschitz Condition for Estimation in Direction of Arrival

Xiuhui Tan, Peng Wang, Hongping Hu, Rong Cheng, Yanping Bai

School of Mathematics, North University of China, Taiyuan, China
Email: tanxiuhui@nuc.edu.cn

Abstract

There are many DOA estimation methods based on different signal features, and these methods are often evaluated by experimental results, but lack the necessary theoretical basis. Therefore, a direction of arrival (DOA) estimation system based on self-organizing map (SOM) and designed for arbitrarily distributed sensor array is proposed. The essential principle of this method is that the map from distance difference of arrival (DDOA) to DOA is Lipschitz continuity, it indicates the similar topology between them, and thus Kohonen SOM is a suitable network to classify DOA through DDOA. The simulation results show that the DOA estimation errors are less than 1° for most signals between 0° to 180°. Compared to MUSIC, Root-MUSIC, ESPRIT, and RBF, the errors of signals under signal-to-noise ratios (SNR) declines from 20 dB to 2 dB are robust, SOM is better than RBF and almost close to MUSIC. Further, the network can be trained in advance, which makes it possible to be implemented in real-time.

Keywords

DOA Estimation, Kohonen SOM, Distance Difference of Arrival, Topological Order, Lipschitz Condition

1. Introduction

Array signal processing is an important branch in the field of modern signal processing, one of the important issues in array signal processing is the estimation of the direction of arrival (DOA). In recent years, many different DOA estimation algorithms have been proposed, including subspace decomposition, sparse decomposition, maximum likelihood parameter estimation, and mapping approximation, etc.

Subspace decomposition *i.e.* eigenspace spectral decomposition is an impor-

tant method for estimation of DOA. It includes several algorithms represented by multiple signal classification algorithm (MUSIC) [1] and Estimation of Signal Parameters via Rotational Invariance Technique (ESPRIT) [2]. In the last few years, many algorithms based on these two algorithms have been proposed [3] [4] [5] [6]. Such as short-time fourier transform-based MUSIC (STFT-MUSIC) [7], real-valued root-MUSIC (RV-root-MUSIC) [8], time-frequency spatial spectral decom-position [9], discrete fourier transform ESPRIT (DFT-ESPRIT) [10], Time-Frequency Multi-Invariance ESPRIT (t-f MI-ESPRIT) [11], neuro-evolution of augmenting topologies MUSIC (RNEAT-MUSIC) [12], and combining ESPRIT with MUSIC [13], etc. These algorithms mainly decompose the signal in observation space into signal subspace and noise subspace using the spectral decomposition of covariance array, and obtain the spectral function based on the property of orthogonality of the two, thus predicting the DOA. The spectral decomposition operation involves the covariance array, which makes this type of algorithm quite computationally intensive, thus is limited from the feasibility of real-time applications.

The sparse representation (SR) and compressive sensing (CS) have become hot spots of research on DOA estimation recently [14] [15]. The theory is originally proposed by Donoho [16] and Candes [17] in 2006. Following that, many DOA estimation algorithms based on sparse algorithms have been proposed, such as matching pursuit (MP) [18], orchogonal matching pursuit (OMP) [19], etc. The initial sparse decomposition method is limited by the density size of the grid, and to solve this limitation, many sparse decomposition methods on off-grid have been proposed [20] [21] [22]. However, this class of algorithms still suffers from practical problems such as large computational effort.

Maximum likelihood parameter estimation uses Gaussian white noise as the noise background, and the maximum value of the likelihood function as the goal for the optimal solution for DOA estimation. The maximum likelihood estimation method is classified into deterministic maximum likelihood (DML) [23] and stochastic maximum likelihood (SML) [24]. Many studies are still being focused on the maximum likelihood estimation algorithm [25] [26]. This method is superior to the subspace decomposition method in the case of low signal-to-noise ratio and small number of snapshots. While the solving process requires a nonlinear multidimensional search, so it suffers from practical problems of high computational effort.

Another type of DOA estimation method is the mapping approximation method. It aims to establish a mapping relationship between the signal observation space and the DOA space, and is typically represented by various neural networks [27] [28], among them the Radial Basis Function Neural Network (RBFNN) [29] and Convolutional Neural Network (CNN) [30] [31] are the representatives. By establishing a nonlinear mapping between the received signal feature vector and the DOA space through a neural network, such methods avoid complex calculations with spectral decomposition. However, there are limitations to the training data. To get the exact mapping from the signal observa-

tion space to the DOA space is a difficult task, so a new solution idea is proposed and initially discussed in the issues of DOA estimation of communication signals [32]. Further, the method is applied to hydroacoustic DOA estimation under a uniform line array [33]. This method discretizes the continuous mapping by finding the mapping relationship between the topological ordering of the array signal time difference of arrival (TDOA) feature space and the topological ordering of the DOA space, so as to build a dictionary with look-up function for estimation of direction of arrival [33]. While it only investigates TDOA features under a specific uniform linear array and fails to provide further discussion on the topological ordering of TDOA features under other types of arrays as well as random arrays, the established mapping matching principles are rough and the estimation results are overly dependent on the density of the training grid.

According to Lipschitz condition, the topological order of the time difference of arrival (TDOA) or distance difference of arrival (DDOA) and the DOA of signals are similar, therefore we propose a discrete DOA estimation system by setting up a two-level SOM neural network. The SOM performs a nonlinear mapping between TDOA and the DOA of signals. It is shown that the system has the advantage of high accuracy, robustness, and implementations. The rest of this paper are organized as following. In section 2, we introduce the arbitrarily distributed sensor array data model, and then we introduce the structure of Kohonen self-organizing map, set up a two-level SOM neural network for the estimation of DOA, and analyze the topological order relationship between DDOA vectors and DOAs in Section 3. In section 4, a simulation study of the proposed system is implemented, the accuracy and feasibility of the proposed method is discussed. Finally, we discuss and conclude the paper in Section 4 and 5.

2. Background Material

Assume that there is a sensor array of M sensors in the 2-D plane as shown in **Figure 1**, the distance between each two adjacent sensors i and $i + 1$ is Δ_i, and
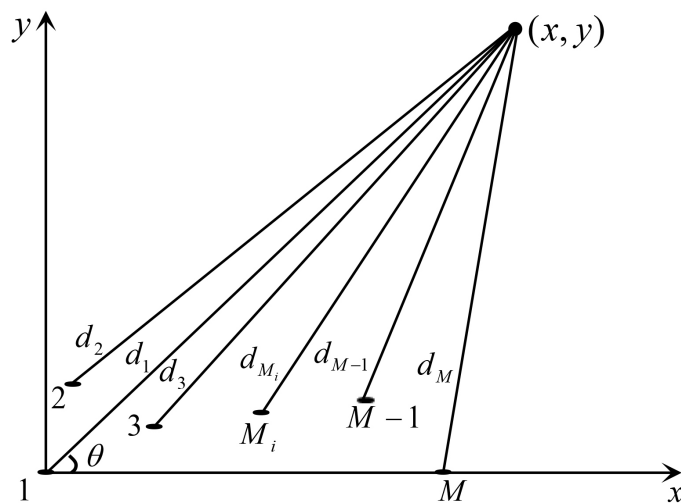

Figure 1. Sensor array and signal source.

$$\Delta_i \le \lambda , \ (i = 1, 2, \cdots, M-1). \tag{1}$$

where λ is the wave length of sound source, and $\lambda = c/f$, where c is the speed of sound wave propagation in a medium, f is the frequency of sound source. Establish rectangular coordinate system, let sensor 1 and M placed on the x-axis, and sensor 1 located at the origin. Suppose that there is a single sound source located at point (x, y) in the plane, and the location of sensor i is $(x_i, y_i) \ (i = 1, 2, \cdots, M)$.

In this paper, the direction of arrival to estimated is the inclination angle of point (x, y) respect to $(0, 0)$, write as

$$\theta = \begin{cases} \arctan\dfrac{y}{x} & x \ge 0, y \ge 0, \\ \pi + \arctan\dfrac{y}{x} & x \le 0, y \ge 0. \end{cases} \tag{2}$$

Let the observations of sensor i be

$$u_i(t) = s(t + t_i) + n_i(t) \ (i = 1, 2, \cdots, M). \tag{3}$$

where $s(t)$ is the signal radiating from the signal source, t_i is the time delay to sensor i, and $n_i(t)$ is the additive noise. We assume that the signal and noises are mutually independent and the noises distribution is Gaussian with zero means, variance of σ^2. The distance from signal source (x, y) to sensor $i \ (i = 1, 2, \cdots, M)$ is written as

$$r_i = \sqrt{(x - x_i)^2 + (y - y_i)^2}, \ (i = 1, 2, \cdots, M). \tag{4}$$

And the distance difference to sensor i and $i + 1$ is

$$\begin{aligned} r_{i,i+1} &= r_{i+1} - r_i \\ &= \sqrt{(x - x_{i+1})^2 + (y - y_{i+1})^2} - \sqrt{(x - x_i)^2 + (y - y_i)^2}, (i = 0, 1, \cdots, M-1) \end{aligned} \tag{5}$$

Then the time difference between sensor i and $i + 1$ is

$$\Delta t_{i,i+1} = r_{i,i+1}/c, \ (i = 0, 1, \cdots, M-1). \tag{6}$$

Thus, TDOA vector noise free is

$$T_0 = \boldsymbol{r}/c = \left[\Delta t_{1,2}, \Delta t_{2,3}, \cdots, \Delta t_{M-1,M} \right]^{\mathrm{T}} \in R^{M-1}, \tag{7}$$

where $\boldsymbol{r} = \left[r_{1,2}, r_{2,3}, \cdots, r_{M-1,M} \right]^{\mathrm{T}}$ is the distance difference vector, and the TDOA vector will be

$$T = T_0 + \boldsymbol{n}. \tag{8}$$

where $\boldsymbol{n}$ represents the noise, which is delay estimation error, and

$$\boldsymbol{n} = \left[n_{1,2}, n_{2,3}, \cdots, n_{M-1,M} \right]^{\mathrm{T}},$$

$$n_{i,i+1} = n_{i+1} - n_i, \ (i = 0, 1, \cdots, M-1). \tag{9}$$

The central question is to set up a map $F : R^{M-1} \to R^1$, from TDOA vector T_0 to DOA θ, *i.e.*

$$\theta = F(T_0), \tag{10}$$

And the estimated parameters θ is to approximate the function

$$\hat{\theta} = \hat{F}(T_0). \tag{11}$$

where $\hat{F}$ denotes an estimation of *F* using neural network.

3. Data Preprocessing by Self-Organizing Map

3.1. Self-Organizing Map

In this paper, we set up a Kohonen self-organizing map, which is also called Kohonen feature map. SOM is a feed-forward neural network, which is an unsupervised and competitive learning algorithm [16]. SOM represent high-dimensional input data as low-dimensional (one- or two-dimensional) data, and keep the same topological order as original data do, thus the features of the input data will be visualizing in an order fashion. The other hand, SOM can be used for feature extraction and dimensionality reduction, too.

A SOM network is composed of two layers: input layer and output layer (competitive layer). As shown in **Figure 2**, there are identical numbers of input layer node to the input vector dimensions, the neurons of competitive layer are usually placed into a two-dimensional grid, which is usually arranged as rectangle or hexagonal. The variable weight connects the input nodes and output node *i* is written as $\omega_i = [\omega_{i1}, \omega_{i2}, \cdots, \omega_{im}]^{\mathrm{T}}$, where *m* is the dimension of the input vector.

Kohonen SOM's training principle is as follows. When an input sample vector is put into the network, the Euclidean distance between neurons weights $\omega_i (i = 1, 2, \cdots, K)$ and the input sample vector are calculated, the one who has the minimum distance will be the winning neuron. Then adjust the weights of the winning neuron and its neighboring neurons, to make them similar to the input sample vector. As a result, all neurons' connected weights have a certain distribution by the training process.

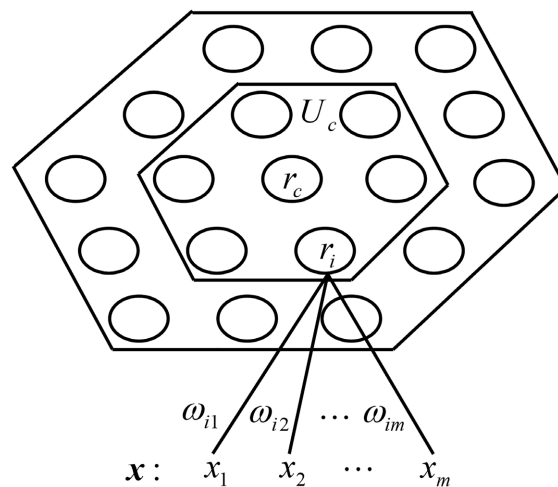The network training process consists of four steps:

Figure 2. Structure of Kohonen self-organizing map.

Step 1: Initialize the network. Assume that there are N sample vectors $x_k \left(k = 0, 1, \cdots, N \right)$, normalize as

$$\tilde{x}_k = x_k / \|x_k\| = x_k \Big/ \left(\sum_{j=1}^{m} x_{kj}^2 \right)^{1/2} . \tag{12}$$

where $x_k = \left[x_{k1}, x_{k2}, \cdots, x_{km} \right]^{\mathrm{T}} \in R^m$. And then give neuron weights ω_i equal to part of the normalized input vector as the initial weights of the network:

$$\omega_i = \tilde{x}_{k_i} \left(i = 1, 2, \cdots, K \right). \tag{13}$$

Step2: Calculate the Euclidean distance between the normalized input vector $\tilde{x}_k$ and each neuron weight ω_i, find the winning neuron ω_c subject to

$$D \left(\tilde{x}_k, \omega_c \right) = \min_i D \left(\tilde{x}_k, \omega_i \right). \tag{14}$$

where

$$D \left(\tilde{x}_k, \omega_i \right) = \sqrt{ \sum_{j=1}^{m} \left(\tilde{x}_{kj} - \omega_{ij} \right)^2 } . \tag{15}$$

Step 3: Adjust the weights of winning neuron c. Adjust nodes i in neighborhood of winning node c, the adjustment is linear combination of input vector and current weight vector:

$$\omega_{ij} \left(t + 1 \right) = \omega_{ij} \left(t \right) + \eta \left(t \right) \left[\tilde{x}_{kj} - \omega_{ij} \left(t \right) \right]$$
$$i \in N_c \left(t \right), \quad \left(j = 0, 1, \cdots, m \right). \tag{16}$$

where $\eta \left(t \right)$ is a decreasing learning rate function of training epoch t, and $N_c \left(t \right)$ is the neighborhood kernel with Gaussian function:

$$U_c \left(t \right) = \exp \left(\|r_j - r_c\|^2 \Big/ 2\sigma^2 \right) \eta \left(t \right). \tag{17}$$

where r is the location of neurons on the two-dimensional grids, and σ is the smoothing factor.

Step 4: Repeat steps 2 and 3 until the convergence criterion is satisfied.

3.2. Lipschitz Condition

If function $\varphi \left(x \right)$ satisfy the following conditions on interval $\left[a, b \right]$:

1) When $x \in \left[a, b \right]$, $\varphi \left(x \right) \in \left[a, b \right]$, *i.e.*, $a \leq \varphi \left(x \right) \leq b$;
2) For any $x_1, x_2 \in \left[a, b \right]$, $\left| \varphi \left(x_1 \right) - \varphi \left(x_2 \right) \right| \leq L \left| x_1 - x_2 \right|$.

It is said that function $\varphi \left(x \right)$ satisfies Lipschitz condition on $\left[a, b \right]$, and $\varphi \left(x \right)$ is Lipschitz continuity, The least constant L for which the previous inequality holds, is called the Lipschitz constant of φ. Lipschitz continuity is a more smoothness condition than uniform continuity. Intuitively, Lipschitz continuous function limits the speed of function change. The slope of a function that meets Lipschitz condition must be less than a real Lipschitz constant, which depends on function φ.

3.3. DOA Estimation with SOM

In this paper, N points in the two-dimensional plane are used to generate train-

ing data. The N points represent the locations of N sound sources, each point corresponds to a distance difference vector r (which is given as Equation (7)) respect to the sensor array. Consider that there is only a constant factor c difference between the DOA vectors T_0 and the distance difference vector r, we use r as an alternative input vector to T_0 as training samples in this issue.

A two-level SOM neural network is set up. As shown in **Figure 3**, the first level of SOM is a mapping from R^{M-1} to R^2, the mapping makes the topological order of training samples visualized in the two-dimensional space. The input vectors are the normalized vectors r in the R^{M-1} space, they are mapped into the K ($K \le N$) nodes on the two-dimensional space. The connection weights are adjusted continuously through automatic competition, and each activated node represents the center of one cluster, the sample vectors which is close enough on Euclidean distance are mapped onto one cluster. At the same time, the adjacent extent of neighboring nodes also reflects the degree of proximity between the input vectors r. It is shown that the two-dimensional map keeps the same topological order with the distance difference vector r.

The second level of SOM we set up is a 1-1 mapping process. It is from the trained two-dimensional space to another two-dimensional space, obviously, they have the same structure and number of nodes. Each node of the second map represents a cluster of angles of arrival, which is obtained according to the location of the signal source that activates the node. Assumed that node i in the first layer is activated by n_i ($\sum n_i = n$) sample vectors, and the coordinates for the corresponding signal source are (x_i, y_i), the direction of arrival corresponding to (x_i, y_i) is θ_i. Consider that the node of the first level may be activated by one, several or none training vectors; the output of second level is constructed as the following rules (**Figure 4**):

1) If node i has been activated by one training input vector, the angle of the corresponding training signal source will be the output, and $\hat{\theta} = \theta_i$.

2) If node i has been activated by not only one training input vector, then the average angles of the corresponding signal sources will be the output as this node stands for, then

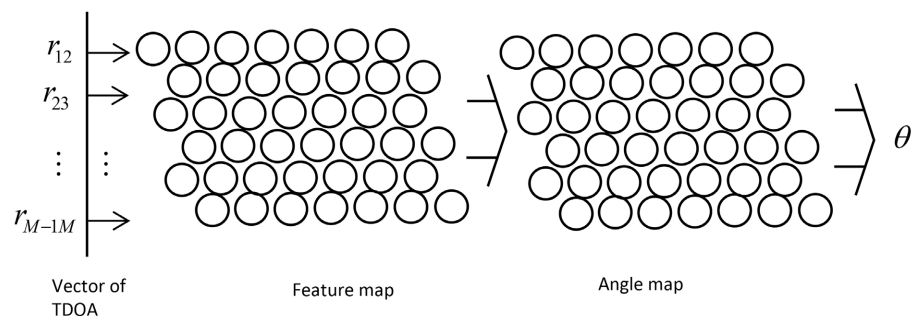$$\hat{\theta} = \frac{1}{n_i} \sum_{k=1}^{n_i} \theta_k . \tag{18}$$

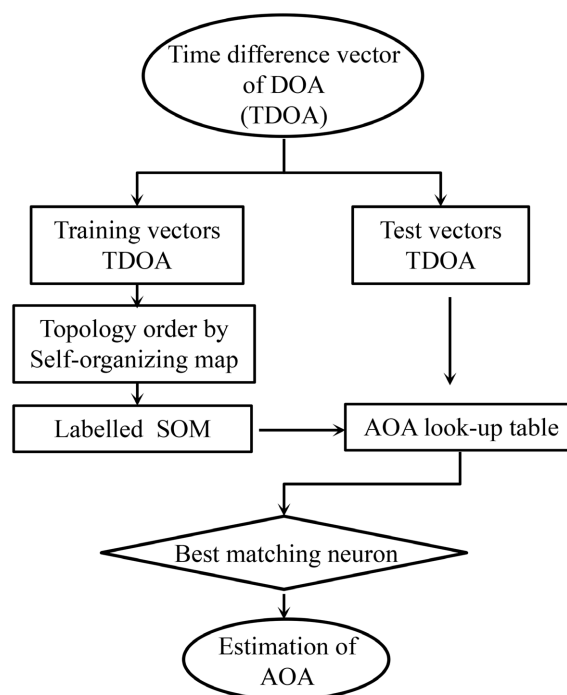**Figure 3.** Two-level SOM.

Figure 4. Flowchart of DOA estimation by the two-level SOM.

3) If node *i* has not been activated by any training input vector, the node will be considered as a null node. When it is activated by a new input vector, the output will be substituted with the value of the nearest one in Euclidean.

The process of DOA estimation we proposed is shown in **Figure 4**. The process is divided into two parts, the train part and test part. The network is trained by a large number of TDOA vectors from a large number of DOAs, through the Kohonen SOM the training vectors are grid up on an two dimensional level in theirs topological order. The DOAs level are arranged directly connected with level one, and keep the same topological order, thus the two level SOM are set up as an labelled network. When there is a new TDOA vector is put into the SOM, an optimal matching node will give the estimation of AOA.

3.4. Analysis of Reliability under Lipschitz Condition

The validity of the proposed method is based on whether the topological order of DOA is the same as (or similar to) vector of DDOA's. In another word, if the Euclidean distance between vectors of DDOA of two signals is small, then the corresponding Euclidean distance between DOAs will be small as well. This is the theoretical basis of our estimation of DOA. Next, we will analysis the conditions it needs to meet.

Let (x, y) be the location of a signal source, another sound source's coordinate is $(x + \Delta x, y + \Delta y)$, where Δx and Δy are small variations. Thus the distance difference vectors of the two signal sources are r and $r_1 = r + \Delta r$, the DOAs of them are θ and $\theta_1 = \theta + \Delta\theta$ respectively. According to Equation (4) and Equation (5), the increment is obtained,

$$\Delta \boldsymbol{r} = \left[\Delta r_{1,2}, \Delta r_{2,3}, \cdots, \Delta r_{M-1,M} \right]^{\mathrm{T}}. \tag{19}$$

Obviously that function $r_{i,i+1}$ is an elementary function and it is differentiable at point $(x, y) \in R^2$, thus

$$\Delta r_{i,i+1} \approx \frac{\partial r_{i,i+1}}{\partial x} \Delta x + \frac{\partial r_{i,i+1}}{\partial y} \Delta y = A_i(x, y)(x\Delta x + y\Delta y). \tag{20}$$

And the Euclidean distance between $\boldsymbol{r}$ and $\boldsymbol{r}_1$ is

$$\left\| \boldsymbol{r}_1 - \boldsymbol{r} \right\| = \left(\sum_{i=1}^{M-1} A_i^2(x, y) \right)^{\frac{1}{2}} \left| x\Delta x + y\Delta y \right|. \tag{21}$$

Since function θ is an elementary function and it is differentiable at point $(x, y) \in R^2 \ (x \neq 0)$, then

$$\Delta \theta \approx \frac{\partial \theta}{\partial x} \cdot \Delta x + \frac{\partial \theta}{\partial y} \cdot \Delta y = B(x, y)(-y\Delta x + x\Delta y). \tag{22}$$

The ratio of the two distances is

$$\frac{\left\| \theta_1 - \theta \right\|}{\left\| \boldsymbol{r}_1 - \boldsymbol{r} \right\|} = D(x, y) \cdot \left| \frac{-y\Delta x + x\Delta y}{x\Delta x + y\Delta y} \right|. \tag{23}$$

when point (x, y) is fixed, $D(x, y)$ is a constant, let

$$R(x, y, \Delta x, \Delta y) = D(x, y) \cdot \left| \frac{-y\Delta x + x\Delta y}{x\Delta x + y\Delta y} \right|.$$

There are three kinds of conditions on R with the changes of Δx and Δy around zero:

1) R is a constant function; assume that $R = R_0$, where R_0 is a constant. Equation 27 will be

$$\frac{\left\| \theta_1 - \theta \right\|}{\left\| \boldsymbol{r}_1 - \boldsymbol{r} \right\|} = R_0, \tag{24}$$

And then

$$\left\| \theta_1 - \theta \right\| = R_0 \left\| \boldsymbol{r}_1 - \boldsymbol{r} \right\|. \tag{25}$$

That is to say the Euclidean distance between DDOA vectors is in proportion to the corresponding Euclidean distance between DOA, $\left\| \boldsymbol{r}_1 - \boldsymbol{r} \right\|$ will change as $\left\| \theta_1 - \theta \right\|$. In this condition, the SOM we set up is absolutely valid to DOA estimation.

2) R is a bounded function; there exists a positive constant L subject to

$$|R| \leq L, \quad (\Delta x, \Delta y) \in (0, a] \times (0, b]. \tag{26}$$

where a, b is a positive constant, that is

$$\frac{\left\| \theta_1 - \theta \right\|}{\left\| \boldsymbol{r}_1 - \boldsymbol{r} \right\|} \leq L \cdot \left\| \boldsymbol{r}_1 - \boldsymbol{r} \right\|. \tag{27}$$

Then

$$\left\| \theta_1 - \theta \right\| \leq L \left\| \boldsymbol{r}_1 - \boldsymbol{r} \right\|. \tag{28}$$

Take the SOM we set up as a function $F: R^{M-1} \to R^1$, *i.e.* $\theta = F(r)$, then

$$\|F(r_1) - F(r)\| \le L\|r_1 - r\|. \tag{29}$$

It shows that function F satisfies Lipschitz conditions, F is uniformly continuous, then for $\forall \varepsilon > 0$, there $\exists \delta > 0$, if only $\|r_1 - r\| < \delta$, then $\|F(r_1) - F(r)\| < \varepsilon$. When the Euclidean distance between DDOA vectors was small enough, the corresponding Euclidean distance between DOA must be very small, too. So, the SOM we set up is also valid to DOA estimation in this condition.

3) R is an unbounded function, in this condition, there are no definitive relationship between $\|r_1 - r\|$ and $\|\theta_1 - \theta\|$, and the SOM we set up will be invalid in estimation of DOA.

In short, when $R(x, y, \Delta x, \Delta y)$ is bounded, TDOA vectors and DOAs will have a similar topological order and distribution, and the SOM we setup can be used in DOA estimation reliably.

4. Simulation Results

4.1. Without Noise

In this section, to verify the effectiveness of the two-level SOM network we setup, simulations are carried out as follow. In the simulations, we assume a sensor array with four sensors, the frequency of sound source is $f = 2\,\text{kHz}$, the speed of sound wave propagation in water is $c = 1500\,\text{m/s}$, and the distance of each two adjacent sensors is set to be $\Delta_i = 0.375$, which is half of the wave length. The sensor positions are $(x_1 = 0, y_1 = 0)$, $(x_2 = 0.3, y_2 = 0.225)$, $(x_3 = 0.5, y_3 = -0.0922)$, $(x_4 = 0.6, y_4 = 0.2692)$. To get training vectors, 60×30 uniform distribution points are taken in rectangular region $[-20, 20] \times [0, 20] \in R^2$ as the positions of 1800 signal sources (**Figure 6**, black points), and then 1800 distance difference vectors r are got as training sample vectors. Calculate $R_{\max}(x, y)$ value,

$$R_{\max}(x, y) = \max_{\substack{0.05 \le \Delta x \le 1 \\ 0.05 \le \Delta y \le 1}} R(x, y, \Delta x, \Delta y),$$

$$(x, y) \in [-100, 100] \times [-100, 100] \tag{30}$$

where $R(x, y, \Delta x, \Delta y)$ is definite as Equation (27). As shown in **Figure 5**, there are a common upper bound for most points (except a few points near $(0, 0)$), belongs the second case, the method we propose is valid.

To test the trained network by signals in different distance and different angles, the locations of 180 test signals are chosen to be on the spiral of Archimedes:

$$\rho = 50\theta, \quad \theta \in [0°, 180°]. \tag{31}$$

On which the DOA changes from 0° to 180°, and the distance changes from 0 to 62.83 (**Figure 6**, green points). The nodes of feature map and DOA map are arranged as 50×50, which is a few more than the training data in number. Put the distance difference vectors of test signals into the trained network, and then get the estimation of DOAs. **Figure 7** is the error of estimation; except several signals most of the error are within $[-1°, 1°]$.
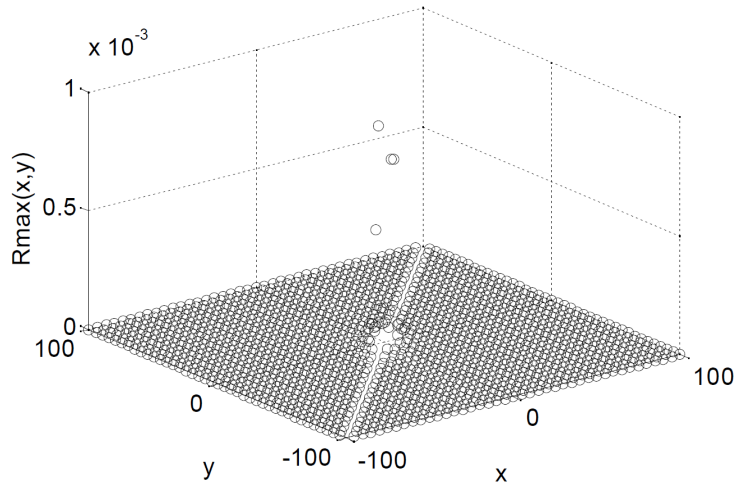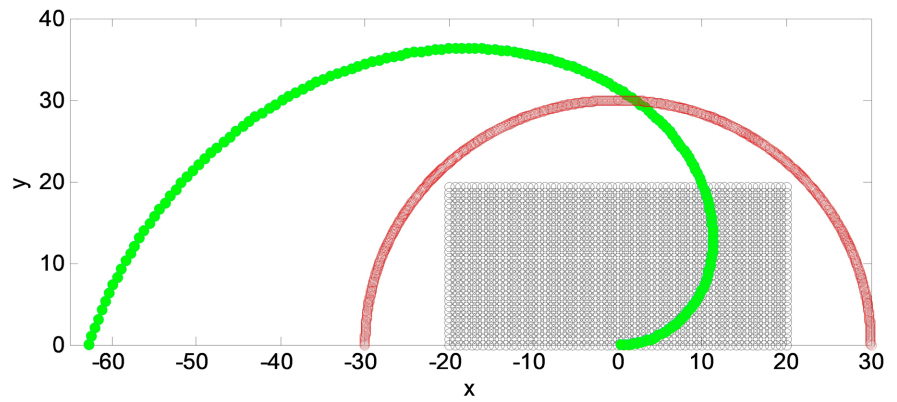
Figure 5. Value of $R_{\max}(x, y)$.

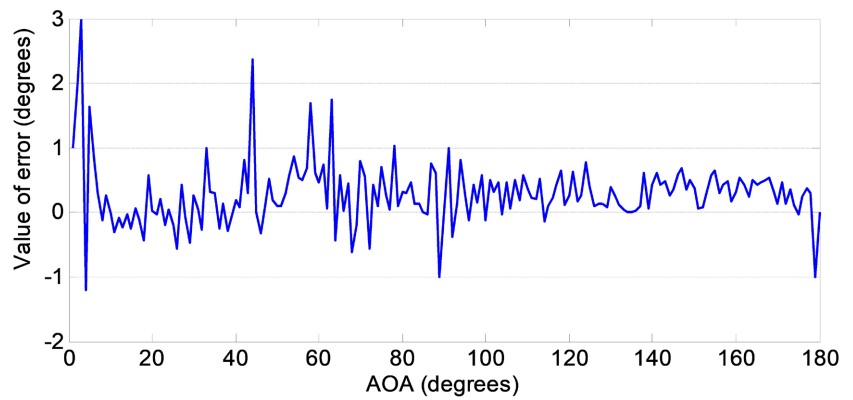**Figure 6.** Training data and test data.

Figure 7. Estimation errors with rectangular region training data.

To test the trained network by signals in different distance and different angles, the locations of 180 test signals are chosen to be on the spiral of Archimedes:

$$\rho = 50\theta, \quad \theta \in \left[0^\circ, 180^\circ\right]. \tag{32}$$

On which the DOA changes from 0˚ to 180˚, and the distance changes from 0 to 62.83 (Figure 6, green points). The nodes of feature map and DOA map are arranged as 50 × 50, which is a few more than the training data in number. Put the distance difference vectors of test signals into the trained network, and then get the estimation of DOAs. Figure 7 is the error of estimation, except several signals most of the error are within $\left[-1^{\circ}, 1^{\circ}\right]$.

From the result above we can see that the results of DOA estimation are mainly associated to the angles of training signals, but little to the localizations. Thus, we chose another group of training data for contrast, a set of signals on circle

$$\rho = 30, \quad \theta \in \left[0^{\circ}, 180^{\circ}\right]. \tag{33}$$

1800 uniform distribution points are taken from the circle (Figure 6, red points). The test signals are the same with above.

At the same time, to study the factor of nodes arrangement, 8 kinds of nodes distributions are evaluated. The average absolute values of estimation error are shown as Table 1. It can be seen that the circle training data performs better than rectangular region, the network with 40 × 40 nodes get better accuracy in DOA estimation, which is a type of $n \times n$ and the number of nodes are a few less than training data, while the other structures performs poor relatively.

4.2. With Gaussian Noise

In practice, there are always additive noises with the signal received by sensor array; therefore, a practical method needs to be robust when noise exists. Take a simulate sinusoidal signal as a sound source, assume that the sound source are located in the direction of 30˚ for example, additive Gaussian noise are added to the signal from a ratio of signal to noise (SNR) of 20 dB to a SNR of 0 dB as Equation (3), then take the DDOA vectors of the 21 noisy signals as test data for the trained network (rectangular region trained). To test the performance of SOM network, we take MUSIC, Root-MUSIC, ESPRIT, and RBF for contrast,

Table 1. Results of DOA estimation by SOM neural network with different nodes arrangement and training data (degree).

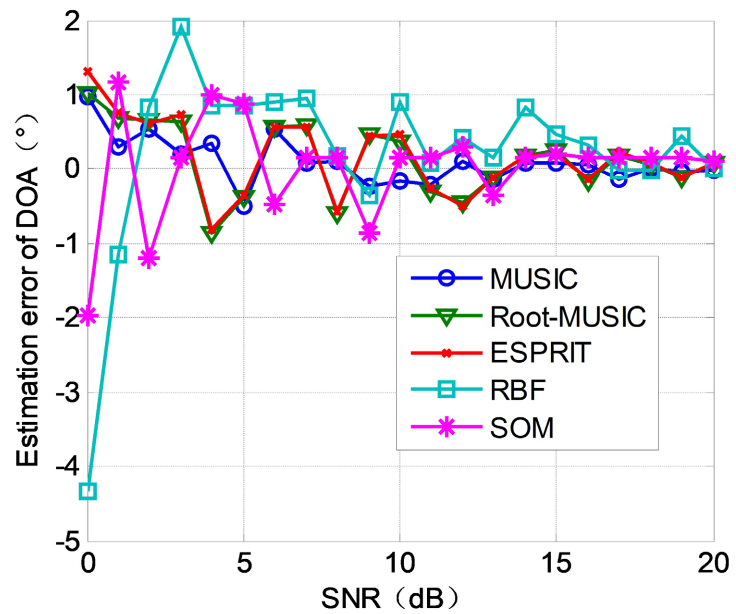| Nodes	Rectangular region	Circle
20 × 20	0.74	0.48
25 × 25	0.52	0.56
30 × 30	0.54	0.35
40 × 40	0.49	0.31
30 × 60	0.57	0.46
40 × 50	0.60	0.54
45 × 45	0.63	0.37
50 × 50	0.68	0.45

Figure 8. Comparison of DOA estimation errors for SOM, MUSIC, Root-MUSIC, ESPRIT, and RBF.

where the RBF neural network take the rectangular region signals' DDOA vectors as input data, and the corresponding DOAs as output to train the network. The DOA estimation errors are as shown in **Figure 8**. When the SNR is higher than 2 dB, the errors of SOM are within 1˚, and change little with the SNR decreases from 20 dB to 2 dB. Compared to MUSIC, Root-MUSIC, ESPRIT, and RBF, SOM performs better than RBF and slightly worse than MUSIC in anti-interference, and almost similar with Root-MUSIC and ESPRIT. Consider that the noises are added to features directly by SOM, in fact, usually the SNR of features should be much high after the process of de-noising, thus the performance of SOM will be much better than as shown in **Figure 8**. It indicates that the system of two-level SOM has the advantages of stability and accuracy and avoids the disadvantage of large calculation in addition.

5. Discussion

The proposed method in this study is an exploratory study of the relationship between characters of signals and DOA, there are many approaches designed for DOA estimation that try different methods of extracting features, and then validate the effectiveness of the accuracy of predicting DOA through different experimental solutions. The basis of this type of research is often supported by data results only, but lacks further deep theoretical discussion.

In this work, we attempt to discussion of the theoretical basis by using Lipschitz condition. When a mapping is Lipschitz continuous, the closer the original images of the mapping are to each other, the closer the images are to each other. For a variety of reasons, the analytic formula for the mapping between some features and DOA cannot be written directly, thus a variety of research

methods for approximating the map based on a finite number of discrete data for fitting are proposed. In this study, we take a direct approach to estimate the Lipschitz coefficients from discrete features through Equation (30). When the maximum value of Lipschitz coefficients in a region is within an acceptable range, then the mapping between features and DOA is considered to be approximately Lipschitz continuous, and DOA estimation can be performed using the principle that similar features correspond to similar DOAs. The next problem comes to how to topologically sort the features, and it can be done by Kohonen self-organizing neural networks. In this work, we estimate DOA by building a two-layer Kohonen self-organizing neural network to perform the tasks used for approximate mapping and query dictionaries.

However, the Lipschitz coefficient estimated using equation 30 in this paper has two limitations. First, this estimation is limited to the sparsity of the sampled signal grid, which is closer to the true value when the grid is more dense and relatively rough when the grid is less dense. Second, the values of the Lipschitz coefficients in the local neighborhoods of different sampling points may vary widely, so the matching estimation DOA errors based on the Kohonen neural network will have a different. As shown in Figure 7, although the global error can be controlled within a certain range, the error range varies widely for different areas of the test points.

6. Conclusion

A two-level SOM system to estimate the DOA based on DDOA vectors was proposed and demonstrated experimentally. The system implements a classifier for DOA through the classification of DDOA vector, which is based on the theory of Lipchitz condition. The error on DOA varied within 1° for the noise free signals from 0° to 180°. The system is robust to noise when the SNR decreased from 20 dB to 2 dB, compared to MUSIC Root-MUSIC, ESPRIT, and RBF, most error of SOM are lower than 1°, and are stable relatively. The methodology avoids calculating the covariance matrix and decomposition, when estimating the DOA, the network can be trained in advance, which makes it feasible to carry out in real-time processing.

Acknowledgements

Conflicts of Interest

The authors declare no conflicts of interest regarding the publication of this paper.

References

[1]   Schmidt, R.O. (1986) Multiple Emitter Location and Signal Parameter Estimation.

IEEE Transactions on Antennas and Propagation, **34**, 276-280.
https://doi.org/10.1109/TAP.1986.1143830

[2] Roy, R. and Kailath, T. (1989) ESPRIT-Estimation of Signal Parameters via Rotational Invariance Techniques. *IEEE Transactions on Acoustics, Speech, and Signal Processing*, **37**, 984-995. https://doi.org/10.1109/29.32276

[3] Meng, F.-X., Li, Z.-T., Yu, X.-T. and Zhang, Z.-C. (2022) Quantum Algorithm for MUSIC-Based DOA Estimation in Hybrid MIMO Systems. *Quantum Science and Technology*, **7**, Article ID: 025002. https://doi.org/10.1088/2058-9565/ac44dd

[4] Li., X. and Zhang, W. (2021) DOA Estimation Using Virtual ESPRIT with Successive Baselines and Coprime Baselines. *Circuits, Systems, and Signal Processing*, **40**, 2065-2075. https://doi.org/10.1007/s00034-020-01560-1

[5] Chen, J., Guan, S., Tong, Y. and Yan, L. (2018) Two-Dimensional Direction of Arrival Estimation for Improved Archimedean Spiral Array with MUSIC Algorithm. *IEEE Access*, **6**, 49740-49745. https://doi.org/10.1109/ACCESS.2018.2867460

[6] Zhou, C. and Zhou, J. (2017) Direction-of-Arrival Estimation with Coarray ESPRIT for Coprime Array. *Sensors*, **17**, Article No. 1779.
https://doi.org/10.3390/s17081779

[7] Zhang, H., Bi, G., Cai, Y., Razul, S.G. and See, C.M.S. (2016) DOA Estimation of Closely Spaced and Spectrally-Overlapped Sources Using a STFT-Based MUSIC Algorithm. *Digital Signal Processing*, **52**, 25-34.
https://doi.org/10.1016/j.dsp.2016.01.015

[8] Yan, F.-G., Shuai, L., Wang, J., Shi, J. and Jin, M. (2018) Real-Valued Root-MUSIC for DOA Estimation with Reduced-Dimension EVD/SVD Computation. *Signal Processing*, **152**, 1-12. https://doi.org/10.1016/j.sigpro.2018.05.009

[9] Cui, K., Wu, W., Huang, J., Chen, X. and Yuan, N. (2017) DOA Estimation of LFM Signals Based on STFT and Multiple Invariance ESPRIT. *AEU-International Journal of Electronics and Communications*, **77**, 10-17.
https://doi.org/10.1016/j.aeue.2017.04.021

[10] Kim, S., Oh, D. and Lee, J. (2015) Joint DFT-ESPRIT Estimation for TOA and DOA in Vehicle FMCW Radars. *IEEE Antennas and Wireless Propagation Letters*, **14**, 1710-1713. https://doi.org/10.1109/LAWP.2015.2420579

[11] Lin, J., Ma, X., Yan, S. and Hao, C. (2016) Time-Frequency Multi-Invariance ESPRIT for DOA Estimation. *IEEE Antennas and Wireless Propagation Letters*, **15**, 770-773. https://doi.org/10.1109/LAWP.2015.2473664

[12] Li, Y., Huang, Y., Pedersen, G.F. and Shen, M. (2022) Recurrent NEAT Assisted 2D-DOA Estimation with Reduced Complexity for Satellite Communication Systems. *IEEE Access*, **10**, 11551-11563. https://doi.org/10.1109/ACCESS.2022.3145583

[13] Liu, A., Li, F., Li, B., Liu, Q. and Shi, X. (2018) Spatial Polarimetric Time-Frequency Distribution-Based DOA Estimation: Combining ESPRIT with MUSIC. *EURASIP Journal on Wireless Communications and Networking*, **2018**, Article No. 51.
https://doi.org/10.1186/s13638-018-1058-9

[14] Fortunati, S., Grasso, R., Gini, F., Greco, M.S. and LePage, K. (2014) Single-Snapshot DOA Estimation by Using Compressed Sensing. *EURASIP Journal on Advances in Signal Processing*, **2014**, Article No. 120.
https://doi.org/10.1186/1687-6180-2014-120

[15] Dai, J., Zhao, D. and Ji, X. (2012) A Sparse Representation Method for DOA Estimation with Unknown Mutual Coupling. *IEEE Antennas and Wireless Propagation Letters*, **11**, 1210-1213. https://doi.org/10.1109/LAWP.2012.2223651

[16] Donoho, D.L. (2006) Compressed Sensing. *IEEE Transactions on Information Theory*, **52**, 1289-1306. https://doi.org/10.1109/TIT.2006.871582

[17] Candès, E.J., Romberg, J. and Tao, T. (2006) Robust Uncertainty Principles: Exact Signal Reconstruction from Highly Incomplete Frequency Information. *IEEE Transactions on Information Theory*, **52**, 489-509. https://doi.org/10.1109/TIT.2005.862083

[18] Cotter, S.F. (2007) Multiple Snapshot Matching Pursuit for Direction of Arrival (DOA) Estimation. *Proceedings of the* 15*th European Signal Processing* (*EUSIPCO* 2007), Poznan, 3-7 September 2007, 247-251.

[19] Wang, W. and Wu, R. (2013) High Resolution Direction of Arrival (DOA) Estimation Based on Improved Orthogonal Matching Pursuit (OMP) Algorithm by Iterative Local Searching. *Sensors*, **13**, 11167-11183. https://doi.org/10.3390/s130911167

[20] Yuan, J., Zhang, G., Leung, H. and Ma, S. (2023) Off-Grid DOA Estimation for Noncircular Signals via Block Sparse Representation Using Extended Transformed Nested Array. *IEEE Signal Processing Letters*, **30**, 130-134. https://doi.org/10.1109/LSP.2023.3242808

[21] Su, X., Liu, Z., Shi, J., *et al.* (2023) Real-Valued Deep Unfolded Networks for Off-Grid DOA Estimation via Nested Array. *IEEE Transactions on Aerospace and Electronic Systems*. https://doi.org/10.1109/TAES.2023.3235746

[22] Shen, J., Gini, F., Greco, M.S. and Zhou, T. (2023) Off-Grid DOA Estimation Using Improved Root Sparse Bayesian Learning for Non-Uniform Linear Arrays. *EURASIP Journal on Advances in Signal Processing*, **2023**, Article No. 34. https://doi.org/10.1186/s13634-023-00991-7

[23] Bohme, J. (1984) Estimation of Source Parameters by Maximum Likelihood and Nonlinear Regression. *ICASSP '84. IEEE International Conference on Acoustics, Speech, and Signal Processing*, San Diego, 19-21 March 1984, 271-274.

[24] Wax, M. (1992) Detection and Localization of Multiple Sources in Noise with Unknown Covariance. *IEEE Transactions on Signal Processing*, **40**, 245-249. https://doi.org/10.1109/78.157206

[25] Rui, L., Liu, X.B. and Chen, X.M. (2023) Localization and Tracking of Multiple Fast Moving Targets in Bistatic MIMO Radar. *Signal Processing*, **203**, Article ID: 108780. https://doi.org/10.1016/j.sigpro.2022.108780

[26] Selva, J. (2023) Efficient Computation of ML DOA Estimates under Unknown Nonuniform Sensor Noise Powers. *Signal Processing*, **205**, Article ID: 108879. https://doi.org/10.1016/j.sigpro.2022.108879

[27] El Zooghby, A.H., Christodoulou, C.G. and Georgiopoulos, M. (2000) A Neural Network-Based Smart Antenna for Multiple Source Tracking. *IEEE Transactions on Antennas & Propagation*, **48**, 768-776. https://doi.org/10.1109/8.855496

[28] Agatonović, M., Stanković, Z., Dončov, N., *et al.* (2012) Application of Artificial Neural Networks for Efficient High-Resolution 2D DOA Estimation. *Radioengineering*, **21**, 1038-1045.

[29] Lo, T., Leung, H. and Litva, J. (1994) Radial Basis Function Neural Network for Direction-of-Arrivals Estimation. *IEEE Signal Processing Letters*, **1**, 45-47. https://doi.org/10.1109/97.300315

[30] Charkrabarty, S. and Habets, E.A.P. (2019) Multi-Speaker DOA Estimation Using Deep Convolutional Networks Trained with Noise Signals. *IEEE Journal of Selected Topics in Signal Processing*, **13**, 8-21. https://doi.org/10.1109/JSTSP.2019.2901664

[31] Liu, Y., Chen, H. and Wang, B. (2021) DOA Estimation Based on CNN for Under-

water Acoustic Array. *Applied Acoustics*, **172**, Article ID: 107594.
https://doi.org/10.1016/j.apacoust.2020.107594

[32] Xu, J., Shen, X., Mark, J.W. and Cai, J. (2007) Mobile Location Estimation for DS-CDMA Systems Using Self-Organizing Maps. *Wireless Communications and Mobile Computing*, **7**, 285-298. https://doi.org/10.1002/wcm.325

[33] Tan, X., Hu, H., Cheng, R. and Bai, Y. (2015) Direction of Arrival Estimation Based on DDOA and Self-Organizing Map. *Mathematical Problems in Engineering*, **2015**, Article ID: 231307. https://doi.org/10.1155/2015/231307